




Chitosan–Starch–Keratin Composites: Improving Thermo-Mechanical and Degradation Properties Through Chemical Modification

Cynthia G. Flores-Hernández^{1,2} · Arturo Colin-Cruz¹ · Carlos Velasco-Santos² · Víctor M. Castaño³ · Armando Almendarez-Camarillo⁴ · Imelda Olivas-Armendariz⁵ · Ana L. Martínez-Hernández² 

© Springer Science+Business Media, LLC 2017

Abstract Chitosan–starch polymers are reinforced with different keratin materials obtained from chicken feather. Keratin materials are treated with sodium hydroxide; the modified surfaces are rougher in comparison with untreated surfaces, observed by Scanning Electron Microscopy. The results obtained by Differential Scanning Calorimetry show an increase in the endothermic peak related to water evaporation of the films from 92 °C (matrix) up to 102–114 °C (reinforced composites). Glass transition temperature increases from 126 °C in the polymer matrix up to 170–200 °C for the composites. Additionally, the storage modulus in the composites is enhanced up to 1614% for the composites with

modified ground quill, 2522% for composites with modified long fiber and 3206% for the composites with modified short fiber. The lysozyme test shows an improved in the degradability rate, the weight loss of the films at 21 days is reduced from 73% for chitosan-starch matrix up to 16% for the composites with 5 wt% of quill; but all films show a biodegradable character depending on keratin type and chemical modification. The outstanding properties related to the addition of treated keratin materials show that these natural composites are a remarkable alternative to potentiating chitosan–starch films with sustainable features.

Keywords Chemical modification · Keratin · Chicken feather · Sodium hydroxide · Biopolymer composite

Electronic supplementary material The online version of this article (doi:[10.1007/s10924-017-1115-1](https://doi.org/10.1007/s10924-017-1115-1)) contains supplementary material, which is available to authorized users.

✉ Ana L. Martínez-Hernández
almh72@gmail.com

¹ Facultad de Química, Universidad Autónoma del Estado de México, Paseo Colon Esq. Paseo Tollocan, 50120 Toluca, Mexico

² División de Estudios de Posgrado e Investigación, Tecnológico Nacional de México, Instituto Tecnológico de Querétaro, Av. Tecnológico s/n Esq. Gral. Mariano Escobedo, Col. Centro Histórico, 76000 Querétaro, Mexico

³ Departamento de Ingeniería Molecular de Materiales, Centro de Física Aplicada y Tecnología Avanzada, Universidad Nacional Autónoma de México, Boulevard Juriquilla 3001, 76230 Querétaro, Mexico

⁴ Departamento de Ingeniería Química, Tecnológico Nacional de México, Instituto Tecnológico de Celaya, Av. Tecnológico y Antonio García Cubas s/n. Celaya, 38010 Guanajuato, Mexico

⁵ Instituto de Ingeniería y Tecnología, Universidad Autónoma de Cd. Juárez, Av. Del Charro 450 Norte, Col. Partido Romero, 32310 Cd. Juarez, Chihuahua, Mexico

Introduction

Fiber-reinforced polymeric composites have been used for a variety of structural applications and are an alternative solution to ever-depleting petroleum sources. The reinforcement of polymer matrices with a growing array of natural fibers is a huge research field under constant development, and new alternatives are created to diversify the properties of natural fibers and green polymer films [1–11].

Natural fibers play an important role in developing high-performance, fully biodegradable “green composites” as environmentally friendly alternatives to synthetic fibers [11–13]. Advantages of natural fibers over traditional reinforcing materials include low cost, low density, good thermal properties, enhanced energy recovery and biodegradability [12, 14, 15]. Also, natural fibers can affect the mechanical properties of bio-matrices [16]. However, the shortcomings of natural fiber-reinforced composites in natural polymer matrices have been their high moisture

absorption, poor wettability and poor fiber–matrix adhesion [15]. To improve the properties of their composites, natural reinforcing fibers can be modified by physical and chemical methods [1, 17].

Natural fibers have hydroxyl groups that allow the fibers to undergo a chemical treatment. Chemical modifications expose more reactive groups on the fiber surface and thus facilitate efficient coupling with the matrix. In recent years, there have been several studies to modify the performance of cellulosic natural fibers [18]. Different surface treatment methods of these fibers have been studied to improve their strength, size and shape, and also the fiber–matrix adhesion [19–27].

One of the most common and efficient methods of chemical modification is alkali treatment of fibers, which has been used to treat almost all natural cellulosic fibers with successful results. It is reported that alkaline treatment has two effects on the fibers: (1) it increases surface roughness, resulting in better mechanical interlocking; and (2) it increases the amount of cellulose exposed on the fiber surface, thus increasing the number of possible reaction sites [28, 29]. Thus, alkali treatment has been considered a good technique to modify the fiber surface to obtain better adhesion between the fiber and the matrix [15]. On the other hand, focus on the reuse of keratin materials obtained from chicken feathers—an alternative to vegetable fibers and a contribution to sustainability—as an alternative reinforcement in composite materials has gained acceptance from many researchers over the last decade [30–38].

Keratin from poultry feathers (the United States poultry industry produces approximately 1.5 billion kg of chicken feathers each year [34]) is a fibrous protein that shows high stability due to its self-assembled hierarchical structure [39]. Chicken feathers have unique structures and properties not found in any other natural or synthetic fibers. The low density, excellent compressibility and resilience, the ability to dampen sound and retain warmth, and the distinctive morphological structure of feather barbs, make them unique fibers [40, 41].

However, research into the use of keratin materials from chicken feathers in composites is mainly focused on synthetic polymers [30, 33, 39, 40] or recently in combination with some synthetic monomers [3] to produce films, and only a few reports have been published on the use of totally natural polymers reinforced by keratin materials obtained from feathers [34–36]. Recently, we reported the development of green composites with keratin materials (short fiber, long fiber and quill) as reinforcements of a chitosan–starch matrix [37]. This report showed evidence of improved mechanical and thermo-mechanical properties in the green composites, due to the good interface and compatibility between the keratin fillers and the polymer matrix. Due to these results, the study presented here utilizes a common

modification method to improve the reported effects in the composites, but now utilizing functionalized keratin fillers.

In the present article, the thermo-mechanical properties of chitosan–starch films are potentiated by developing composites with chemically modified keratin materials. Thus, the aim of this study is to contribute an explanation of the effect of chemical treatment in the thermal and mechanical properties of keratin as reinforcement in a natural matrix, and also to improve notably the development of this type of sustainable composite elaborated with natural polymers. In addition, lysozyme degradation tests are realized in order to verify the changes produced in chitosan–starch through the incorporation of keratin materials (short fiber, long fiber and ground quill) without treatment, and after chemical modification. Thus, in spite of a common modification method is used for keratin material, the results have been not been reported before, and the notable improvements of natural polymeric matrix composites could be useful in extending the potential uses of these types of material. The enhanced properties of green polymers are important alternatives to be applied and to produce possible benefits for the environment.

Materials and Methods

Materials

Chitosan (85% deacetylated) was obtained from Sigma-Aldrich. Potato starch was purchased from National Starch, Co. (Hammond, IN, USA). Sorbitol was acquired from Golden Bell Reactivos, acetic acid was obtained from J.T. Baker and chicken feathers were supplied by Pilgrim's Company (Queretaro, Mexico). The reagent grade (>98%) sodium hydroxide employed in this work was purchased from Sigma-Aldrich.

Preparation of Keratin Biofibers and Ground Quill

Feathers, as obtained from Pilgrim's, were washed with water and ethanol and dried in order to be clean, white, sanitized and odor-free. The keratin biofibers (barbs and barbules) were separated from the quill by cutting manually; these are called long biofibers (L). Short biofibers (S) were obtained when the long biofibers were finely milled in a hammer mill. Also the quill (GQ) was milled in a hammer mill (Pulvex, model 200, sieve 4 mm).

Sodium Hydroxide (NaOH) Treatment

Keratin biofiber was placed in a glass vessel and 100 mL NaOH 0.1 M was added to the vessel and stirred well. Keratin biofiber was immersed for 5 h and heated to 50 °C. Then, the alkaline-treated biofibers were washed thoroughly in

plenty of distilled water to remove the excess NaOH (pH 11). Thereafter, the fibers were dried at 35 °C for 48 h (fiber humidity 9.2%) before the composites were made. Chemical conditions to modify keratin materials were elected taking into account previous unpublished work; the conditions described here produce changes in the surface of the keratin materials but the keratin structure was unaffected.

Composite Preparation

Table 1 shows the corresponding concentrations and nomenclature used in the synthesis and characterization of composites. All the films were obtained by the casting/solvent evaporation method previously described by Flores-Hernandez et al. [37]. The composites reinforced with four different contents (5, 10, 15 and 20 wt%) of treated short and long keratin biofibers and ground quill were prepared for this investigation. The resulting mixture was poured into poly(tetrafluoroethylene) dishes to complete gel formation and later was cooled to 35 °C (film humidity 9.4%) for 96 h. All treatments were carried out in duplicate.

Lysozyme Tests

To evaluate the composite degradation a solution 1 L of phosphate buffer solution (PBS) was prepared with the following quantities: 8 g NaCl, 0.20 g KCl, 0.14 g KH₂PO₄, 0.91 g Na₂PO₄. Reagents were added one by one in distilled water with stirring until completely dissolved and adjusted to pH 7.4 using 1 N NaOH and/or 1 N HCl. NaN₃ (0.02%) was added to the buffer solution before sample incubation. Composites for the lysozyme tests were cut, to approximately 1.0 × 1.0 cm. The samples were produced in quadruplicate, and weighed prior to mixing with PBS pH 7.4. The degradation in vitro was conducted in test tubes containing 5 mL PBS with NaN₃ and 5 µg mL⁻¹ of lysozyme. The composites were placed in test tubes and incubated for different periods of time (1 day, and 1, 2, and 3 weeks) at 37 °C. After completing the incubation time of each sample, polymer films were washed with deionized water and dried in a vacuum

oven at room temperature and weighed again. The degradation was evaluated according to the weight loss.

Characterization Methods

Dynamical-mechanical analysis (DMA) was measured using a Perkin-Elmer DMA 8000 under the flexural mode of testing. The dimension of the specimens was 22 × 5 × 0.18 mm. The heating rate was set at 5 °C min⁻¹ and the samples were tested between 30 and 250 °C. Differential scanning calorimetry (DSC) was conducted in a TA Instruments model Q200; samples were heated at a rate of 10 °C min⁻¹ from 15 to 400 °C under nitrogen atmosphere. Two samples of each composite were analyzed for thermal and thermomechanical characterization. The morphology of the composites was observed by scanning electron microscopy (SEM) using a JSM-6060LV JEOL microscope at an accelerating voltage of 20 kV. Samples of all composites were fractured using a Zwick/Roell Z005 universal testing machine, to observe by SEM the behavior of the reinforcement in the matrix. Fractured samples were mounted on metal stubs and vacuum-coated with gold at 7 × 10⁻² mB using argon in a sputter coater EMS 550. The samples obtained after Lysozyme testing were prepared in the same manner for observation by SEM, and the morphological changes during degradation examined; these samples were analyzed using a JSM-7000F JEOL microscope at an accelerating voltage of 5 kV.

Results and Discussion

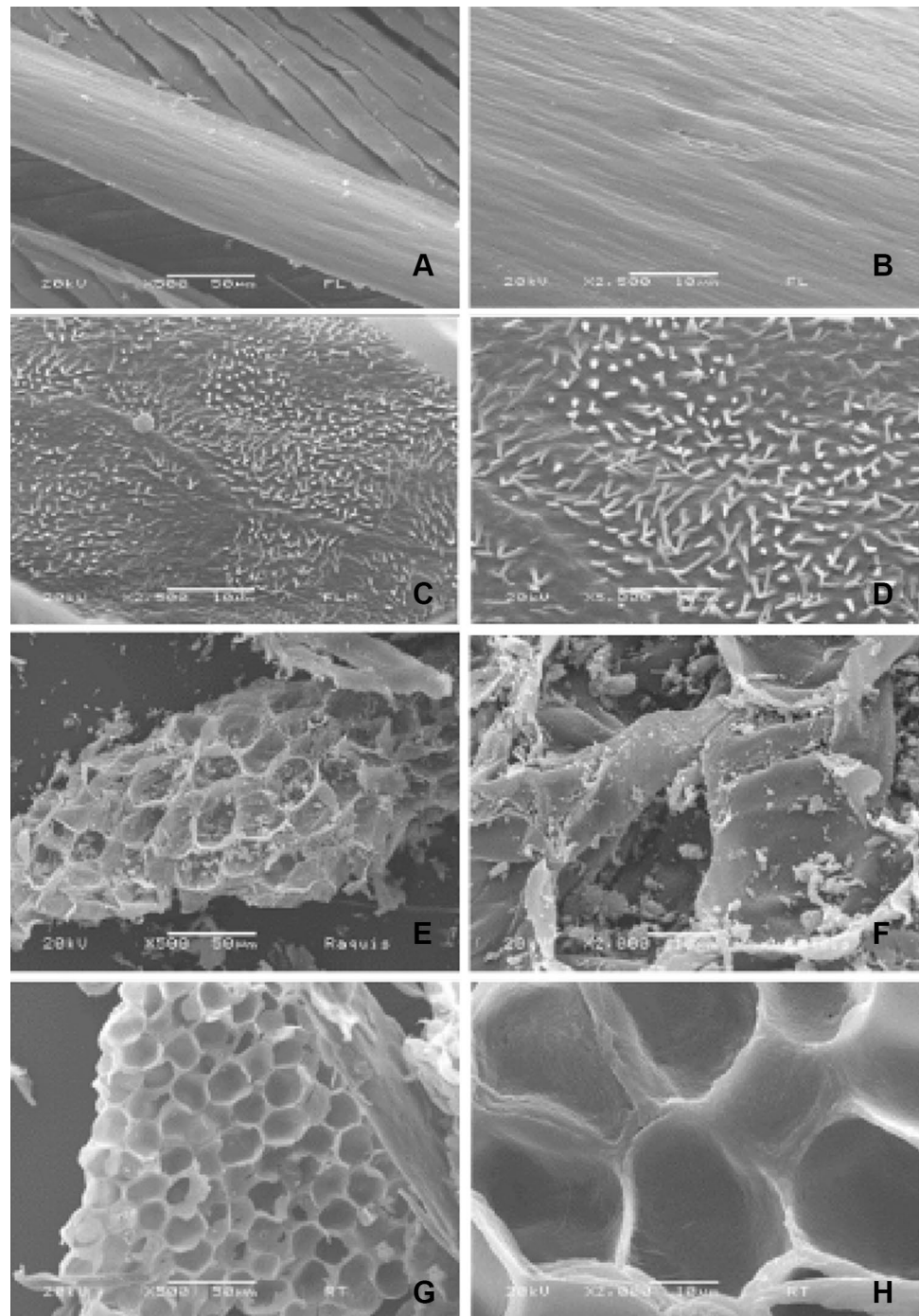
Morphology of Chemical Modification of Keratin Biofibers Studied by Scanning Electron Microscopy

The difference between the keratin biofiber and ground quill before and after alkali treatment is shown in Fig. 1a–h. The SEM micrographs show the clear difference between the surface of the untreated and treated biofibers. The untreated biofibers (Fig. 1a, b) have a smooth longitudinal surface; this surface is completely changed by the chemical treatment with sodium hydroxide. Figure 1c, d shows that the biofiber

Table 1 Composition and nomenclature of chitosan–starch/keratin reinforced composites

Percentage of reinforcement (wt%)	Type of keratin reinforcement					
	Keratin reinforcement			Modified keratin reinforcement		
	Long biofiber	Short biofiber	Ground quill	Long biofiber	Short biofiber	Ground quill
5	ChS-LB05	ChS-SB05	ChS-GQ05	ChS-LM05	ChS-SM05	ChS-GQM05
10	ChS-LB10	ChS-SB10	ChS-GQ10	ChS-LM10	ChS-SM10	ChS-GQM10
15	ChS-LB15	ChS-SB15	ChS-GQ15	ChS-LM15	ChS-SM15	ChS-GQM15
20	ChS-LB20	ChS-SB20	ChS-GQ20	ChS-LM20	ChS-SM20	ChS-GQM20

Fig. 1 Scanning electron microscopy (SEM) micrographs. Surface appearance of long keratin biofiber (LB), **a, b** without treatment; **c, d** with chemical modification of NaOH; and ground quill (GQ), **e, f** without treatment; **g, h** with chemical modification of NaOH



surface has the appearance of tiny fibers, so that a rough surface is revealed. Mercerization of vegetable biofibers has been found to change the surface topography of the fibers and improve tensile strength, flexural strength and impact resistance due to chemical modification [15, 42–44].

The chemical treatment on the surface of the ground quill was carried out to improve compatibility with the chitosan–starch matrix. The alkali treatment dissolves and

leaches out the fatty acids and their condensation products that form the waxy cuticle layer.

The untreated fibers, Fig. 1e, f, show a surface with impurities. The treated ground quill, Fig. 1g, h, shows a very clean surface and also a flat surface without impurities. Also, some studies of cellulosic fibers [45] have shown that the surface of the alkali-treated fiber appears to be quite smooth; however, this keratin fiber is roughened due to the chemical

treatment, and the surface topography shows the absence of surface impurities, which were present on the untreated fiber.

Fiber Dispersion and Physical Appearance of Composites

Figures S1, S2 and S3 shows the composites reinforced with untreated and treated keratin materials. The composites with long biofiber, shown in the images S2 (a–d), exhibit a fiber saturation, which is more evident with increased reinforcement percentage; this is attributed to the length of the fiber, which is not conducive to being completely wetted by the matrix. However, the composites reinforced with treated keratin biofiber S2 (e–h) do not show saturation; thereby achieving a better dispersion. Thus, the modification of the surface of the keratin fiber improves compatibility with the matrix in the case of the long-fiber reinforcement.

Composites reinforced with short biofibers and ground quill (Figs. S1 and S3 respectively) have the same behavior observed in Fig. S2, showing better compatibility and dispersion in composites with modified materials than in those developed with untreated keratin.

Morphology of Composites Studied by Scanning Electron Microscopy

Figure 2 shows the micrographs obtained by scanning electron microscopy of fracture surfaces after tensile tests of chitosan–starch composites reinforced with treated fiber and quill. The fractured surface shows irregularities in its morphology and it can be observed that the fibers are adhered to the matrix. Also, it is possible to observe that there is no separation of phases between the matrix and the reinforcement, and the fibers are completely wetted by the matrix, indicating that the films have a good interaction. In addition,

few voids are found on the fracture surface, because the fibers are trapped by the matrix [37].

Differential Scanning Calorimetry

The basic principle underlying this technique is that when the sample undergoes a physical transformation such as a phase transition, a quantity of heat will need to flow, relative the reference, to maintain both samples at the same temperature. Whether less or more heat must flow to the sample depends on whether the process is exothermic or endothermic [46]. The endothermic and exothermic peaks obtained from differential scanning calorimetry (DSC) for untreated and treated short-fiber keratin, and the composites reinforced with treated short keratin biofiber are shown in Fig. 3. Also in the figure are the thermograms of chitosan–starch and composite with 5 wt% untreated fiber.

The thermogram of the untreated keratin short fiber (SB) shows the following endothermic peaks: (a) around 95 °C related to water evaporation [33, 41, 47, 48]; (b) 227 °C, due to crystalline melting of the fiber keratin [48], specifically assigned to α -helix denaturation of keratin intermediate filaments (KIFs) [47, 49], defined as low sulfur-content keratin, having molecular weights of 60–45 kDa; (c) 247 °C, related to protein denaturation, but explicitly with the formation of inorganic compounds containing sulfur, such as SCS, SCO, H₂S and SO₂ [33, 50]; (d) 290 °C, related to the melting/degradation of keratin associated proteins (KAPs) of the inter-macrofibrillar matrix, defined as high sulfur-content keratin with molecular weights of 28–11 kDa [51]. In the same Fig. 3 is shown the thermogram of keratin short fiber after modification (SM), where it is observed that the zone of water evaporation presents three endothermic peaks, which are related to the hydrophilic behavior acquired by keratin after treatment; it is supposed that this hydrophilic behavior allows division of the water liberation from the keratin into

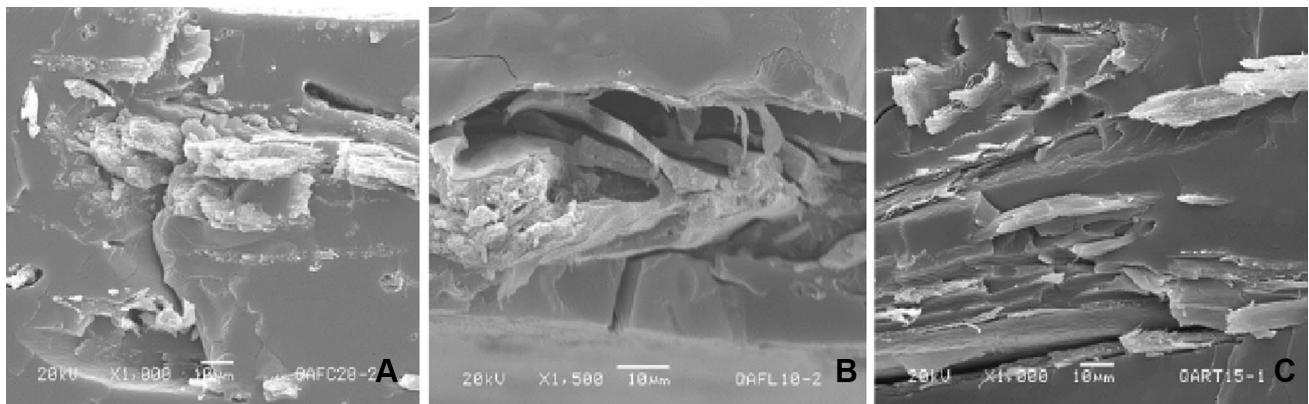


Fig. 2 Scanning electron microscopy (SEM) micrographs of fractured surfaces of chitosan–starch composites reinforced with treated short fiber (a), treated long fiber (b) and ground quill (c)

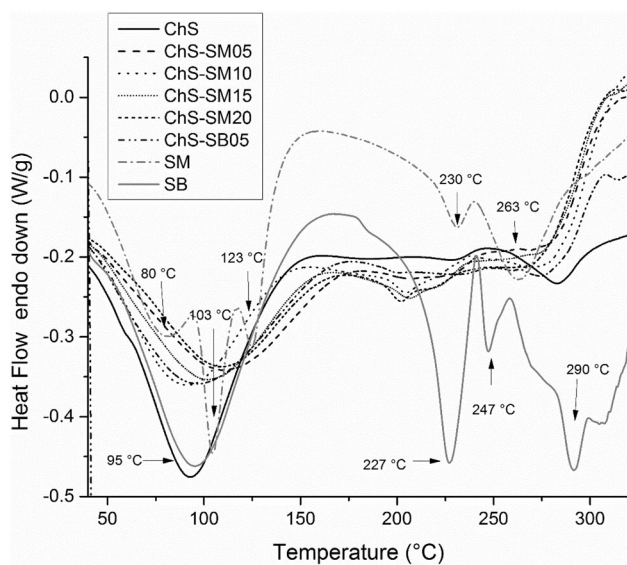


Fig. 3 Differential scanning calorimetry (DSC) curves for composites (ChS-SM), with 5–20 wt% of treated biofiber in comparison with matrix (ChS) and composite with 5 wt% of untreated short biofiber (ChS-SB05). DSC of short fiber untreated (SB) and treated (SM) are included for comparison

three types: “free water”, “loosely bound water” and “chemically bound water” [41]; this latter type of water is related to more bound water in the structure, associated with the peak at higher temperature, 123 °C. In the zone of denaturation of KIF, the peak is shifted slightly to higher temperature compared to the SB thermogram; however in the zone of melting of KAPs the temperature shifts to lower values in comparison to untreated keratin (SB). Similar results have been found for other types of keratin after oxidation with hydrogen peroxide [52]. Thus, it is evident that chemical treatment with NaOH (in this research) or oxidation by other chemical treatments [52] produce comparable degradation of the surface structure; in this case some inter-macrofibrillar matrix segments are diminished or deteriorated. However, the melting temperature of the intermediate filaments is not affected by treatment. Similar behavior is observed in unmodified and modified quill (GQ and GQM). The DSC curves are included in Fig. S4.

Figure 3 also shows the thermograms of chitosan–starch matrix, and the composites with untreated and treated short fiber. In the sample of chitosan–starch, the endothermic peak around 88–100 °C corresponds to the evaporation of water from the film, as has been reported earlier [37, 53, 54]; the same peak is also shown for all composites. Due to increased hydrophilic behavior of treated keratin, which increases with chemical treatment, a slight increase in water evaporation temperature is observed in the majority of the composites with treated short fiber in comparison to matrix and composites with untreated keratin. The second stage in these

thermograms is shown only in the composites; therefore, it corresponds to the crystalline melting temperature of keratin [37, 47, 49, 55] and is more visible in composites with modified keratin. In the third zone, the endothermic peak is attributed to a complex process, including the rupture of the saccharide rings and decomposition of the acetylated and deacetylated units [53]. According to the DSC peaks, it can be deduced that the keratin changes this behavior, and the peak of the third zone is only slightly visible in the composite with untreated keratin, however in the composites reinforced with treated keratin different behavior is presented. This change is related to the effect that produce modified short fibers in the matrix. Thus different materials are produced after treatment. Other studies with natural fibers (hemp) [56] have concluded that alkali treatment improves the thermal stability of the fibers.

For the composites reinforced with ground quill and long fibers, both chemically modified, the behavior was the same, with some shifts in water evaporation temperature and modification of the final degradation of the chitosan–starch due to the effect of the chemically modified keratin. In supplementary information, DSC results for ChS-GQM and ChS-LM composites are included in Figs. S4 and S5, respectively.

Dynamical Mechanical Analysis

DMA can be described as applying an oscillating force to a sample and analyzing the material’s response to that force. In DMA, a complex modulus (E^*), an elastic modulus (E') and an imaginary (loss) modulus (E'') are calculated from the material response to the sine wave. These different moduli allow better characterization of the material because it is possible to analyze the ability of the material to storage energy (E'), to lose energy (E''), and the ratio of these effects ($\tan \delta$), which is called damping [57, 58].

Figure 4a–c shows the comparison of the storages modulus curves of the matrix, the reinforced composites with keratin materials and the composite reinforced with 5 wt% of the keratin material without chemical treatment. It is clear that the storage modulus for all samples with chemically treated long fiber increase significantly with respect to the matrix and the composite with untreated fiber (Fig. 4a). Considering the storage modulus (E') at 38 °C for the matrix and the highest modulus for the composite with 20 wt% of chemically treated long fiber, E' is improved by a factor of 26.2 (2522%), and considering the composite with untreated fibers at the same temperature, by a factor of 4.8 (383%). It is important to mention that the composite with 5 wt% of untreated long fiber is the composite than reached the highest value of storage modulus considering the same concentrations as presented here (5, 10, 15 and 20 wt%), as previously published [37]. Also it is possible to observe that these composites with chemically treated fiber have a

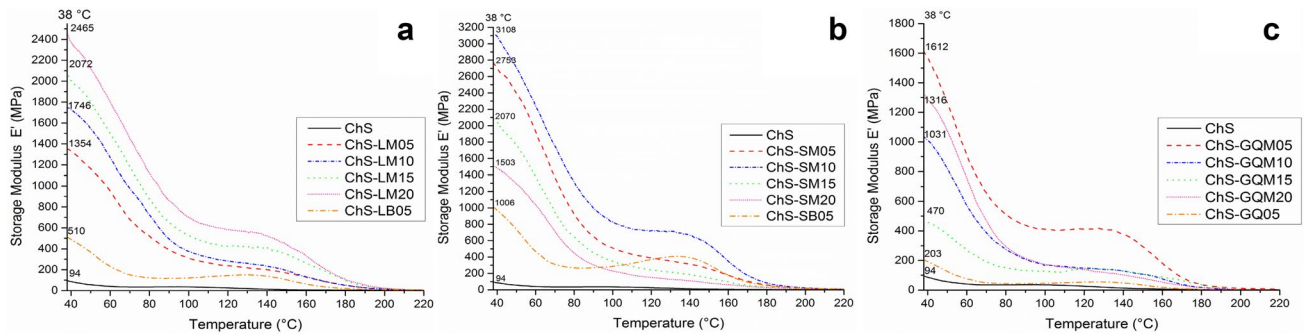


Fig. 4 Storage modulus (E') for composites with 5–20 wt% of treated long biofiber (a), treated short biofiber (b) and treated grounded quill (c)

clear tendency with respect to the quantity of reinforcement used; for example the composite with 5 wt% of reinforcement (ChS-LM05) showed an E' of 1354 MPa, improved by a factor approximately of 14 when compared to the matrix, and the composite with 20% of reinforcement (ChS-LM20) reached an E' of 2465 MPa. Thus, it is evident that this treatment improves significantly the interface between keratin fiber and chitosan–starch; hence, long keratin fibers, after chemical modification, represent an important option for the reinforcement of natural chitosan–starch polymers, in order to improve significantly their thermomechanical properties.

On the other hand, the highest storage modulus ($E' = 3108$ MPa) was obtained with the composite with 10 wt% of chemically-treated short fiber (Fig. 4b), with relevant increases by a factor of 33 (3206%) over the matrix. The E' had a tendency to increase with 5 and 10 wt% of reinforcements (2753, 3108 MPa respectively). It is important to emphasize that all composites with modified fiber showed a better performance than matrix composite ($E' = 94$ MPa) and reinforcement with untreated keratin (1006 MPa), so it is clear that chemical treatment of short fiber also notably improves the storage modulus. DMA results for ChS-GQM are shown in Fig. 4c. The behavior of these materials is very similar to the previously described materials (chemically-modified short and long fiber composites), inasmuch as the composites with chemically modified quill show outstanding values, superior to the matrix and the unmodified fiber composite. However, the values of E' for ChS-MGQ films do not show a clear tendency with respect to the quantity of reinforcement used, but these composites improve by a factor of 17.1 (1614%) when compared to the matrix and by a factor of 7.9 (694%) considering the composite with untreated ground quill at the same temperature. Thus, a good interface and an improved stiffness of chitosan–starch are shown by all keratin materials characterized. Good interface in polymer composites reinforced with natural materials has been reported with increases in storage modulus (E') in different research [45, 59, 60], due to this module being very

sensitive to changes in structure or fiber matrix interface bonding in composites [60].

The term T_g is the reversible transition in amorphous materials (including amorphous regions within semi-crystalline materials) from a molten or rubberlike state into a hard and relatively brittle, glassy state. T_g values are useful for a variety of purposes; for example, they could be used as a function of composition in binary polymer blends, of the effects of fillers in polymers, and of nanoconfinement effects on segmental motions in polymer composites, among others [61, 62]. In DMA the maximum of tan delta is related to T_g . For chitosan–starch composites T_g has been reported to be around 90–100 °C [63].

DMA results also show the T_g values (tan delta maximum) for chitosan–starch matrix to be around 126 °C, and for composite with 5 wt% untreated short fiber, 163 °C. It is important to emphasize two behaviors: (1) Tan delta (T_g) maximums for composites with chemically treated short fiber do not show the same bell behavior as do the matrix and the composite with untreated short fiber. Also, the behavior of these curves (T_g) are different compared to any composite developed with untreated keratin at the same percentages, as previously published [37], and (2) Tan delta maximums for composites with treated short fiber are shifted to higher temperatures (approximately 170–200 °C), indicating that the interaction between matrix and treated fiber changes the movement of the chains, generating a more thermally stable film. The shifts in tan delta are associated with improving the interactions at interface level between reinforcements and matrix [59, 60].

Composites with treated long fiber (ChS-LM) reached maximums of tan delta in the region of 200–240 °C, whereas the composites with treated ground quill shifted the temperature of the maxima to the region 170–180 °C. The thermal change in ChS-LM is associated with decreasing mobility of the polymer chain, indicating that long fibers are able to affect the segmental motions of the polysaccharide chains [37].

The absence of bell behavior but the displacement of the maximum point to a higher temperature suggests that the chemical modification is an important option in the reinforcement of polysaccharide polymers in order to increase their thermomechanical properties. Tan delta curves for all composites are shown in the supplementary information Figs. S6, S7 and S8 for short fiber, long fiber and ground quill, respectively.

Fourier Transform Infrared Analysis

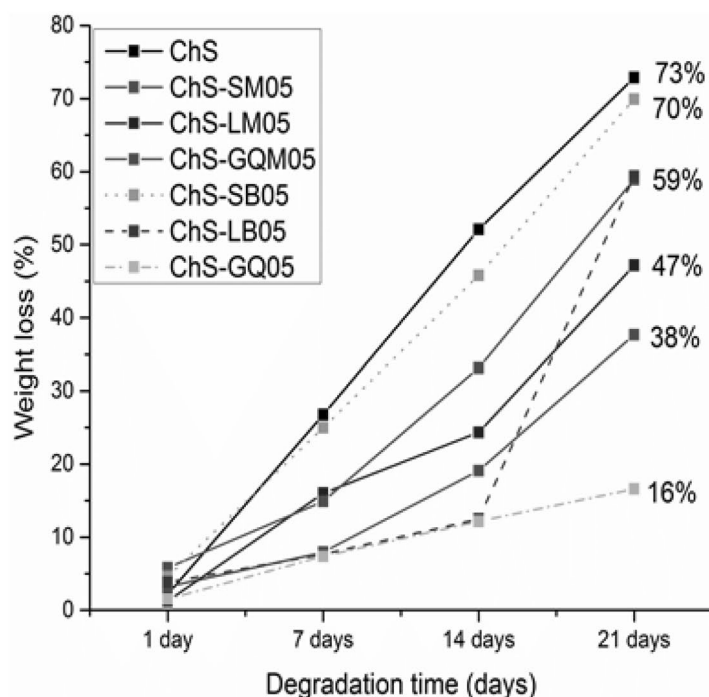
The FTIR in the zone $1800\text{--}800\text{ cm}^{-1}$ for keratin, chitosan–starch films, composites reinforced with short fiber (20 wt%) and composites synthesized with 20 wt% of modified keratin materials can be observed in Fig. S9. In this region, three peaks appear, associated with the matrix between 995 and 1150 cm^{-1} , and are assigned to C–O bond stretching [64]. Also, these peaks appear at the same wavenumber as the peaks of reinforced composite. It is observed that the shoulder found at 1020 cm^{-1} for the composites reinforced with keratin materials increases slightly from that in the matrix spectrum; this band is attributed to interactions of C–O–C bond stretching in saccharide films with hydrogen bonds [37, 64]. In addition, the main peaks related to keratin are detected at 1430 , 1550 and 1630 cm^{-1} . The peak at 1430 cm^{-1} is attributed to the CH_3 group, the next region around $1530\text{--}1550\text{ cm}^{-1}$ is assigned to in-plane bending of

NH group and the band at 1630 cm^{-1} corresponds to the C=O group [37, 41].

Lysozyme Test

The decomposition rate of the chitosan–starch matrix, composites with 5 wt % untreated keratin and composites reinforced with 5 wt% chemically treated keratin were investigated by monitoring the change in weight loss during degradation in phosphate buffer solution at pH 7 and $37\text{ }^\circ\text{C}$. Figure 5 shows the weight loss of these materials. An increasing trend in weight loss is observed from the first to the third week of incubation in PBS. The chitosan–starch films showed the highest percentage of decomposition in this time.

At the end of the three weeks degradation process, the weight loss of matrix was 72%, the highest percentage of decomposition. Composites reinforced with short (SM05), long (LM05) and chemically-treated ground quill (GQM05) showed weight losses of 38, 47 and 59%, respectively. On the other hand, the composites reinforced with untreated fillers, short fiber (SB05), long fiber (LB05) and ground quill (GQ05) experienced weight losses of 69, 59 and 17%, respectively. These results show that all composites with keratin materials are more resistant to degradation than is the matrix. Chemical treatment retards the degradation process in short- and long-fiber reinforced composites, but quill composites are more stable to degradation before chemical



	Standard deviation			
	1 day	7 days	14 days	21 days
ChS	1.17	2.49	1.94	2.51
ChS-SB05	2.31	2.66	2.14	6.18
ChS-LB05	1.16	1.35	0.41	4.45
ChS-GQ05	0.43	2.21	0.65	1.28
ChS-SM05	1.43	1.53	1.21	3.03
ChS-LM05	0.5	1.2	3.68	3.95
ChS-GQM05	4.14	3.56	3.9	2.65

Fig. 5 Lysozyme degradation of ChS films alone and in composites reinforced with keratin: alkali treated and untreated

treatment. Also, Fig. 5 shows the standard deviation that represents the range of variation in experimental data. It can be seen that deviations do not significantly influence the clear changes in film degradation. Considering each type of keratin, only short-fiber (SB05) shows a similar tendency in weight loss to the chitosan–starch matrix. However, the other keratin materials present significant differences in weight loss from the matrix. It is important to note that each reinforcing material has a different behavior with respect to weight loss. Therefore, the length, keratin material structure, orientation, shape and chemical treatment of reinforcements are very significant factors influencing the degradation of the films. Thus, keratin materials produce composites more stable to degradation in chitosan–starch materials, but sustainable behavior is maintained.

Figure S10 shows SEM images obtained after the Lysozyme test. After 3 weeks, it is possible to observe that chitosan–starch films present a different degradation process from those reinforced with untreated keratin. Whereas chitosan–starch films present a segmentation process, and the material get more porosity during the degradation time, composites with untreated keratin (Fig. S10b–d) have less surface roughness after the degradation process, with exception of the sample ChS-SB05, which presents a porous surface polymer matrix; this agrees with the lysozyme degradation curves (Fig. 5). In addition, composites containing treated keratin (Fig. S10e–g) have, since the initial process, a flaky structure that is maintained during the weeks and with different features from the composites containing untreated keratin. Thus, it is observed that degradation of these composites is integral, and keratin materials in the matrix produce new materials, with different characteristics from chitosan starch; therefore, as is observed in the images, keratin, depending on its nature and modification, produces different behavior in these materials.

Conclusions

Environmentally friendly composites made of chitosan–starch and chemically treated keratin materials were obtained. Chemical modification of the keratin materials changed their surface morphology and produced in the composites excellent dispersion and wettability, as observed by the naked eye and in SEM micrographs. This compatibility was reflected in the relevant thermo-mechanical properties achieved, which improve significantly the possible applications of natural matrices. The contributions to the storage modulus of the matrix by the different keratin materials followed this order: SM > LM > GQM.

The relevant interaction of keratin materials was also reflected in the thermal properties of the composites, inasmuch as important changes related to water release by

composites, degradation of saccharide rings and Tg were observed with treated keratin in comparison to the matrix and to composites reinforced with untreated keratin, indicating that materials with different features were produced.

FTIR revealed some possible hydrogen-bond interactions between the reinforcements and the C–O bonds of the matrix. The lysozyme test showed that chemical treatment of keratin, in short and large fibers, retarded the degradation in the composites, and the keratin materials in general gave materials more stable to degradation. SEM after degradation showed different structure degradation in composites with treated keratin compared to untreated keratin composites and matrix.

Chemical treatment of the forms of keratin—short fiber, long fiber and ground quill—changed significantly the behavior and properties of chitosan–starch films compared to untreated keratin, and potentiates their possible applications. The composite materials synthesized with by-products of the poultry industry and the natural biodegradable polymers produced are totally sustainable. These composites hold promise for their potential applications and could be used as films in food packaging material due to their excellent thermo-mechanical and biodegradable properties.

Acknowledgements The authors are grateful to Mrs. Alicia del Real-Lopez for her technical assistance with SEM micrographs, to Dr. Pedro Salas for technical support and Mrs. Carmen Vazquez for assistance in stress tests of the composites (useful to SEM). Also, C.G. Flores-Hernandez thanks Consejo Nacional de Ciencia y Tecnología (CONACyT), Mexico, for financial support through the Ph. D. scholarship. Martinez-Hernandez and Velasco-Santos also express their gratitude for the economic support provided by Tecnológico Nacional de México and Instituto Tecnológico de Querétaro through the projects 2499.09-P and QRO-IMA-2012-103, respectively.

Compliance with Ethical Standards

Conflict of interest The authors declare no conflict of interest.

References

1. Vilaseca F, Mendez JA, Pelach A, Llop M, Cañigueral N, Girones J, Turon X, Mutje P (2007) *Process Biochem* 42:329–334
2. Xu H, Yan Y (2014) *ACS Sustain Chem Eng* 2:1404–1410
3. Shi Z, Reddy N, Hou X, Yang Y (2014) *ACS Sustain Chem Eng* 2:1849–1856
4. Wool RP, Sun XS (2005) *Bio-based polymers and composites*. Elsevier Academic Press, London
5. O'Donnell A, Dweib MA, Wool RP (2004) *Compos Sci Technol* 64:1135–1145
6. Shenton III HW, Wool RP, Hu B, O'Donnell A, Bonnaillie L, Can E, Chapas R, Hong C (2002) *Adv Build Technol* 1:255–262
7. Dweib MA, Hu B, Shenton III HW, Wool RP (2006) *Compos Struct* 74:379–388
8. Hinchcliffe SA, Hess KM, Srubar III WV (2016) *Compos B* 95:346–354

9. Castro DO, Passador F, Ruvolo-Filho A, Frollini E (2017) *Compos A* 95:22–30
10. Khan Z, Yousif BF, Islam M (2017) *Compos B* 116:186–199
11. Goda K, Sreekala MS, Gomes A, Kaji T, Ohgi J (2006) *Compos A* 37:2213–2220
12. Joseph S, Oommen Z, Thomas S (2006) *J Appl Polym Sci* 100:2521–2531
13. Bambach MR (2017) *Thin-Walled Struct* 119:103–113
14. Li X, Tabil LG, Panigrahi S (2007) *J Polym Environ* 15:25–33
15. Cao Y, Shibata S, Fukumoto I (2006) *Compos A* 37:423–429
16. Avella M, Buzarovska A, Errico ME, Gentile G, Grozdanov A (2009) *Materials* 2:911–925
17. Chang WP, Kim KJ, Gupta RK (2009) *Compos Interface* 16:937–951
18. Farsi M (2012) In: Wang J (ed) *Some critical issues for injection molding*. InTech, Rijeka
19. Anike DC, Onuegbu TU, Ogbu IM, Alaekwe IO (2014) *Am J Polym Sci* 4:117–121
20. Kabir MM, Wang H, Lau KT, Cardona F (2012) *Compos B* 43:2883–2892
21. Calado V, Barreto DW, D’Almeida JRM (2000) *J Mater Sci Lett* 19:2151–2153
22. Zheng YT, Cao DR, Wang DS, Chen JJ (2007) *Compos A* 38:20–25
23. Idicula M, Boudenne A, Umadevi L, Bos L, Candau Y, Thomas S (2006) *Compos Sci Technol* 66:2719–2725
24. Ray D, Rana AK, Bose NR, Sengupta SP (2005) *J Appl Polym Sci* 98:557–563
25. Sreekala MS, Thomas S (2003) *Compos Sci Technol* 63:861–869
26. Martins MA, Forato LA, Mattoso LHC, Colnago LA (2006) *Carbohydr Polym* 64:127–133
27. Keener TJ, Stuart RK, Brown TK. (2004) *Compos A* 35:357–362
28. Li X, Panigrahi SA, Tabil LG, Crerar WJ (2004) *The society for engineering in agricultural, food, and biological systems*. In: 2004 CSAE/ASAE Annual Intersectional Meeting, paper Number MB04–305
29. John MJ, Anandjiwala RD (2008) *Polym Compos* 29:187–207
30. Jimenez-Cervantes Amieva E, Velasco-Santos C, Martinez-Hernandez AL, Rivera-Armenta JL, Mendoza-Martinez AM, Castaño VM (2014) *J Compos Mater* 9:1–9
31. Dweib MA, Hu B, O’Donnell A, Shenton HW, Wool RP (2004) *Compos Struct* 63:147–157
32. Hong CK, Wool RP (2005) *J Appl Polym Sci* 95:1524–1538
33. Martinez-Hernandez AL, Velasco-Santos C (2011) In: Dullart R, Mousques J (eds) *Keratin: structure, properties and applications*. Nova Science Publishers, Inc., Hauppauge
34. Cheng S, Lau K, Liu T, Yongqing Z, Lam P, Yin Y (2009) *Compos B* 40:650–654
35. Barone JR (2009) *J Polym Environ* 17:143–151
36. Ozmen U, Baba BO (2017) *J Therm Anal Calorim* 129:347–355
37. Flores-Hernandez CG, Colin-Cruz A, Velasco-Santos C, Castaño VM, Rivera-Armenta JL, Almendarez-Camarillo A, Garcia-Casillas PE, Martinez-Hernandez AL (2014) *Polymers* 6:686–705
38. Rodriguez-Gonzalez C, Martinez-Hernandez AL, Castaño VM, Kharissova OV, Ruoff RS, Velasco-Santos C (2012) *Ind Eng Chem Res* 51:3619–3629
39. Martinez-Hernandez AL, Velasco-Santos C, de-Icaza M, Castaño VM (2007) *Compos B*, 38:405–410
40. Reddy N, Yang Y (2007) *J Polym Environ* 15:81–87
41. Martinez-Hernandez AL, Velasco-Santos C, de-Icaza M, Castaño VM (2005) *Int J Environ Pollut* 23:162–178
42. Das M, Chakraborty D (2006) *J Appl Polym Sci* 102:5050–5056
43. Van de Weyenberg I, Truong TC, Vangrimde B, Verpoest I (2006) *Compos A* 37:1368–1376
44. Pickering KL, Beckermann GW, Alam SN, Foreman NJ (2007) *Compos A* 38:461–468
45. Aziz SH, Ansell MP (2004) *Compos Sci Technol* 64:1219–1230
46. Wunderlich B (2005) *Thermal analysis of polymeric materials*. Springer, New York
47. Khosa MA, Ullah A (2014) *J Hazard Mater* 278:360–371
48. Ullah A, Wu J (2013) *Macromol Mater Eng* 298:153–162
49. Colucci G, Aluigi A, Tonin C, Bongiovanni R (2014) *Prog Org Coat* 77:1104–1110
50. Brebu M, Spiridon I (2011) *J Anal Appl Pyrol* 91:288–295
51. Park M, Shin HK, Panthi G, Rabbani MM, Alam AM, Choi J, Chung HJ, Hong ST, Kim HY (2015) *Int J Biol Macromol* 76:45–48
52. Zhang Q, Shan G, Cao P, He J, Lin Z, Huang Y, Ao N (2015) *Mat Sci Eng C* 47:123–134
53. Mathew S, Brahmakumar M, Abraham TE (2006) *Biopolymers* 82:176–187
54. Goulart SG, De Souza DA, Machado JC, Hourston DJ (2000) *J Appl Polym Sci* 76:1197–1206
55. Balaji S, Kumar R, SriPriya R, Kakkar P, Vijaya Ramesh D (2012) *Mat Sci Eng C* 32:975–982
56. Sreekala MS, Kumaran MG, Thomas S (1997) *J Appl Polym Sci* 66:821–835
57. Menard KP (2008) *Dynamic mechanical analysis: a practical introduction*, 2nd edn. CRC Press, Boca Raton
58. Brostow W, Hagg Lobland HE, Narkis M (2011) *Polym Bull* 67:1697–1707
59. Pothan LA, Thomas S, Groeninckx G (2006) *Compos A* 37:1260–1269
60. Jacob M, Francis B, Thomas S, Varughese KT (2006) *Polym Compos* 27:671–680
61. Kalogeras IM, Hagg Lobland HE (2012) *J Mater Educ* 34:69–94
62. Brostow W, Chiu R, Kalogeras IM, Vassilikou-Dova A (2008) *Mater Lett* 62:3152–3155
63. Lazaridou A, Biliaderis CG (2002) *Carbohydr Polym* 48:179–190
64. Mitrus M (2005) *Int Agrophys* 19:237–241